Available online at www.sciencedirect.com
SCIENCE DIRECT®
ELSEVIER
Journal of Magnetism and Magnetic Materials 271 (2004) 9–26
Journal of magnetism and magnetic materials
www.elsevier.com/locate/jmmm

# On the computation of the demagnetization tensor for uniformly magnetized particles of arbitrary shape. Part I: Analytical approach

S. Tandon[a], M. Beleggia[b], Y. Zhu[b], M. De Graef[a,*]

[a] *Department of Materials Science and Engineering, Carnegie Mellon University, 5000 Forbes Avenue, Pittsburgh, PA 15213-3890, USA*
[b] *Materials Science Department, Brookhaven National Laboratory, Upton, NY 11973, USA*

Received 17 July 2003; received in revised form 24 August 2003

**Abstract**

A Fourier space formalism based on the shape amplitude of a particle is used to compute the demagnetization tensor field for uniformly magnetized particles of arbitrary shape. We provide a list of explicit shape amplitudes for important particle shapes, among others: the sphere, the cylindrical tube, an arbitrary polyhedral shape, a truncated paraboloid, and a cone truncated by a spherical cap. In Part I of this two-part paper, an analytical representation of the demagnetization tensor field for particles with cylindrical symmetry is provided, as well as expressions for the magnetostatic energy and the volumetric demagnetization factors.


*PACS:* 41.20.Gz; 75.30.Gw; 75.40.Mg

*Keywords:* Demagnetization tensor field; Shape amplitude; Magnetometric demagnetization tensor; Demagnetization energy

## 1. Introduction

The computation of demagnetization factors (either volumetric, ballistic, or point function) is an old and difficult problem, with the earliest work going back to the 19th century. All demagnetization factors can be derived from the demagnetization point function or demagnetization tensor field (DTF), so that this tensor field, represented by the symmetric second-rank tensor $N_{ij}(\mathbf{r})$, is the central quantity to be determined. The DTF describes how the magnetic field, $\mathbf{H}(\mathbf{r})$, depends on location for a uniformly magnetized particle with a given shape. It is well known that for the ellipsoid, the DTF is constant inside the body, so that this shape is particularly useful for experimental measurements in a uniform applied field. For other shapes, the DTF depends on position inside the body, so that the interpretation of experiments becomes much more complicated [1].

*Corresponding author. Tel.: +1-412-268-8527; fax: +1-412-268-7596.
*E-mail address:* degraef@cmu.edu (M. De Graef).

0304-8853/$ - see front matter © 2003 Elsevier B.V. All rights reserved.
doi:10.1016/j.jmmm.2003.09.011

Recently, we proposed [2] a new method for the computation (analytical or numerical) of the DTF for a uniformly magnetized particle with an arbitrary shape. The mathematical details of this model are summarized in Section 2. The method expresses all magnetostatic quantities in Fourier space, and employs the concept of the *shape amplitude*, $D(\mathbf{k})$, which is the Fourier transform of the characteristic (or shape) function, $D(\mathbf{r})$. The shape function is constant and equal to 1 inside the particle, and vanishes everywhere outside the particle. In Ref. [2], the model was applied to the derivation of the DTF for a uniformly magnetized sphere, a well-known result, and also to the DTF of a uniformly magnetized tetrahedron. In the present two-part paper, we present additional applications of the Fourier space formalism for the computation of the DTF. In this paper, Part I, we focus our attention on analytical computations, whereas the companion paper, Part II [3], deals with several numerical methods.

The central function in the Fourier space description of the DTF is the shape amplitude $D(\mathbf{k})$. Because of its importance, we provide a number of explicit expressions for the shape amplitude in Section 3. The list includes: the sphere, the cylindrical tube, an arbitrary polyhedral shape (with a rectangular prism, the tetrahedron, and a hexagonal plate as examples), the truncated paraboloid, and a cone with a spherical cap. This list should serve as a guideline for the computation of the shape amplitude for other, more complex particle shapes. In Section 4, we describe first the general theory for the DTF of an object with cylindrical symmetry (4.1), followed by the explicit analytical computation of the DTF for the cylinder (4.2). In Section 5, we compute the magnetostatic energy of the uniformly magnetized cylinder with arbitrary aspect ratio, followed in Section 6 by the computation of the magnetometric (volume-averaged) demagnetization factors for the cylinder. We conclude this paper with a number of applications of the model (Section 7) for the computation of the field at particular locations in space around a solenoid.

## 2. Summary of the theoretical model

In this section, we will repeat briefly the most important conclusions of Ref. [2]. Consider a uniformly magnetized particle with characteristic function (or shape function) $D(\mathbf{r})$ and magnetization $\mathbf{M}(\mathbf{r}) = M_0\hat{\mathbf{m}}D(\mathbf{r})$, where the hat indicates a unit vector and $M_0$ is the saturation magnetization. Using a Fourier space formalism, it can be shown that the magnetic induction, $\mathbf{B}$, inside and around the particle is given by

$$\mathbf{B} = \mu_0(\mathbf{M} + \mathbf{H}) = \mu_0\mathbf{M} - \frac{B_0}{8\pi^3}\int \mathrm{d}^3\mathbf{k}\frac{D(\mathbf{k})}{k^2}\mathbf{k}(\hat{\mathbf{m}}\cdot\mathbf{k})\mathrm{e}^{\mathrm{i}\mathbf{k}\cdot\mathbf{r}}, \tag{1}$$

where the shape amplitude $D(\mathbf{k})$ is equal to the Fourier transform of $D(\mathbf{r})$, and $B_0 = \mu_0 M_0$. The demagnetization field $\mathbf{H}$ is therefore defined as

$$\mathbf{H} = -\frac{M_0}{8\pi^3}\int \mathrm{d}^3\mathbf{k}\frac{D(\mathbf{k})}{k^2}\mathbf{k}(\hat{\mathbf{m}}\cdot\mathbf{k})\mathrm{e}^{\mathrm{i}\mathbf{k}\cdot\mathbf{r}}, \tag{2}$$

If we define the demagnetization tensor $N_{ij}$ by the following relation:

$$B_i = \mu_0(M_i - N_{ij}M_j), \tag{3}$$

then we find an explicit expression for the tensor by comparison with Eq. (1):

$$N_{ij}(\mathbf{r}) \equiv \frac{1}{8\pi^3}\int \mathrm{d}^3\mathbf{k}\frac{D(\mathbf{k})}{k^2}k_i k_j \mathrm{e}^{\mathrm{i}\mathbf{k}\cdot\mathbf{r}}, \tag{4}$$

or, in Fourier space:

$$N_{ij}(\mathbf{k}) = \frac{D(\mathbf{k})}{k^2}k_i k_j. \tag{5}$$

This definition of the demagnetization tensor automatically satisfies the condition that the trace of $N_{ij}$ must be equal to unity inside the particle, and vanish outside. In other words, the trace of the demagnetization tensor field is equal to the shape function, or

$$\mathrm{Tr}[N_{ij}(\mathbf{r})] = D(\mathbf{r}), \tag{6}$$

as shown explicitly in Eq. (7) of Ref. [2]. Furthermore, the shape amplitude can be used to derive expressions for the demagnetization energy, $E_m$, and the average demagnetization tensor inside the particle:

$$E_m = \frac{\mu_0 M_0^2}{16\pi^3} \int \mathrm{d}^3\mathbf{k} \frac{|D(\mathbf{k})|^2}{k^2} (\hat{\mathbf{m}} \cdot \mathbf{k})^2; \tag{7}$$

$$\langle N \rangle_{ij} = \frac{1}{8\pi^3 V} \int \mathrm{d}^3\mathbf{k} \frac{|D(\mathbf{k})|^2}{k^2} k_i k_j. \tag{8}$$

The shape amplitude of a particle without inversion symmetry is a complex quantity, hence the modulus-squared in both of the above integrals.

In Ref. [2], we have applied Eqs. (4), (7), and (8) to the simple case of the uniformly magnetized sphere, for which these results are well known. In the present paper, we will exploit these same expressions for the analytical computation of $N_{ij}(\mathbf{r})$, $E_m$, and $\langle N \rangle_{ij}$ for the finite cylinder. We will also show how a large class of particle shapes with cylindrical symmetry can be dealt with. While the standard analytical computation of $N_{ij}$ requires two volume integrations (6 integrals) within the Fourier space formalism (essentially two 3D Fourier transforms), it is possible to formally integrate four of those integrals for a general object with cylindrical symmetry. This will be done in Section 4.1. Then we apply the general equation to the special case of the finite cylinder and explicitly obtain expressions for all three quantities mentioned above. We begin this paper with a list of shape amplitude functions for important particle shapes.

## 3. Shape amplitudes for important particle shapes

Since the shape amplitude $D(\mathbf{k})$ is the central function for the determination of demagnetization factors and magnetostatic energies, it is useful to list here explicit shape amplitudes for a number of important shapes. Unless mentioned otherwise, the coordinate origin is at the center of the particle. Cartesian coordinates are labeled $(k_x, k_y, k_z)$, cylindrical coordinates $(k_\perp, \theta, k_z)$, and spherical coordinates $(k, \theta, \varphi)$.

- *Sphere*: For a sphere of radius $R$ and volume $V = \frac{4\pi}{3}R^3$ (Fig. 1a), the shape amplitude is given by [4]:

$$D(\mathbf{k}) = \frac{3V}{kR} j_1(kR), \tag{9}$$

  with $j_1(x)$ the spherical Bessel function of the first kind.
- *Cylindrical tube*: For a tube with inner radius $R_1$, outer radius $R_2$, height $2d$, and volume $V = 2d\pi(R_2^2 - R_1^2)$ (Fig. 1b), the shape amplitude is

$$D(\mathbf{k}) = \frac{2V\,\mathrm{sinc}(dk_z)}{k_\perp(R_2^2 - R_1^2)} [R_2 J_1(k_\perp R_2) - R_1 J_1(k_\perp R_1)], \tag{10}$$

  with $J_1(x)$ the Bessel function of the first kind, and $\mathrm{sinc}(x) \equiv \sin(x)/x$. A more general expression for particle shapes of arbitrary cylindrical symmetry is given in Section 4.1.

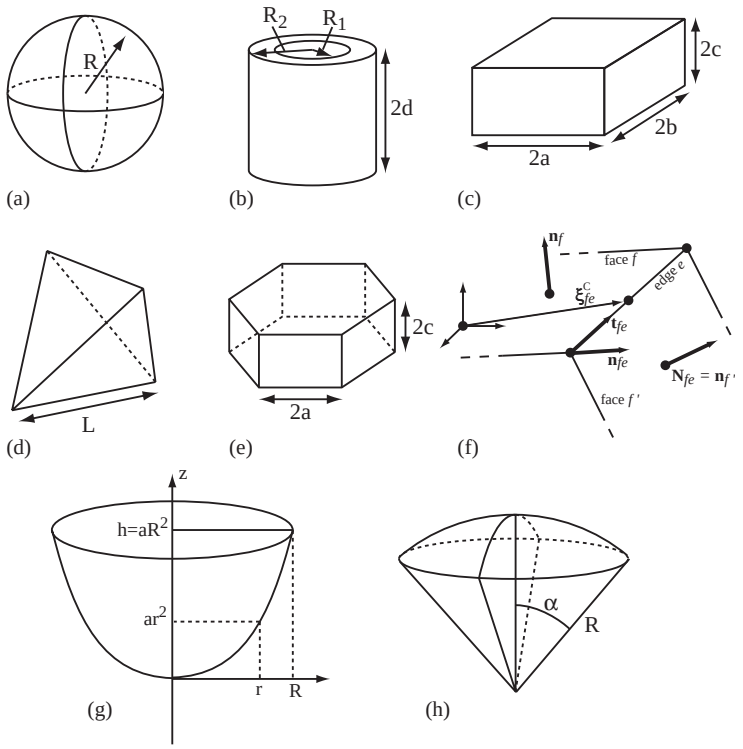


Fig. 1. Schematic representation of the various particle shapes used in Section 3 to derive analytical expressions for the shape amplitude $D(\mathbf{K})$.

- *General polyhedral shape*: The general expression of the shape amplitude for an arbitrary polyhedral particle was derived by Komrska [5].

$$D(\mathbf{k}) = -\frac{1}{k^2}\sum_{f=1}^{F}\frac{\mathbf{k}\cdot\mathbf{n}_f}{k^2-(\mathbf{k}\cdot\mathbf{n}_f)^2}\sum_{e=1}^{E_f}L_{fe}\mathbf{k}\cdot\mathbf{n}_{fe}\operatorname{sinc}\left(\frac{L_{fe}}{2}\mathbf{k}\cdot\mathbf{t}_{fe}\right)\mathrm{e}^{-\mathrm{i}\mathbf{k}\cdot\boldsymbol{\xi}^C_{fe}}. \tag{11}$$

This equation is only valid if the second denominator is non-zero. If $\mathbf{k} = \pm k\mathbf{n}_f$ (in other words, if $\mathbf{k}$ is parallel to any one of the face normals), then the contribution of that particular face (or faces) must be replaced by

$$D_f(\mathbf{k}) = \mathrm{i}\frac{\mathbf{k}\cdot\mathbf{n}_f}{k^2}P_f\mathrm{e}^{-\mathrm{i}d_f\mathbf{k}\cdot\mathbf{n}_f}, \tag{12}$$

where $P_f$ is the surface area of the face $f$, and $d_f$ the distance between the origin and the face $f$. In the origin of Fourier space, the shape amplitude is equal to the particle volume, i.e. $D(\mathbf{0}) = V$. The symbols in Eq. (11) are illustrated in Fig. 1f and defined as: $\boldsymbol{\xi}^C_{fe}$, coordinate vectors of the center of the edge $e$ of face $f$; $\mathbf{n}_f$, unit outward normal to face $f$; $L_{fe}$, length of the $e$th edge of the $f$th face; $\mathbf{t}_{fe}$, unit vector along the $e$th edge of the $f$th face, defined by

$$\mathbf{t}_{fe} = \frac{\mathbf{n}_f\times\mathbf{N}_{fe}}{|\mathbf{n}_f\times\mathbf{N}_{fe}|},$$

where $\mathbf{N}_{fe}$ is the unit outward normal *on* the face which has the edge $e$ in common with the face $f$; $\mathbf{n}_{fe}$, unit outward normal *in* the face $f$ on the edge $e$ defined by $\mathbf{n}_{fe} = \mathbf{t}_{fe}\times\mathbf{n}_f$.

The input parameters needed to complete this computation for an arbitrary polyhedron are the $N_v$ vertex coordinates $\boldsymbol{\xi}_v$ and a list of which vertices make up each face (counterclockwise when looking towards the polyhedron center). All other quantities can be computed from these parameters. The following three shape amplitudes are derived by means of the general shape amplitude for a polyhedral particle.

- *Rectangular prism*: for a rectangular prism with dimensions $2a$, $2b$, $2c$, and volume $V = 8abc$ (Fig. 1c), we have (oriented with edges parallel to cartesian coordinate axes)

$$D(\mathbf{k}) = V\mathrm{sinc}(ak_x)\mathrm{sinc}(bk_y)\mathrm{sinc}(ck_z). \tag{13}$$

- *Regular tetrahedron*: for a regular tetrahedron with edge length $L$ and volume $V$ (Fig. 1d), the shape amplitude is given by [6]:

$$D(\mathbf{k}) = -6\mathrm{i}V[E(a,a,a) + E(a,-a,-a) + E(-a,a,-a) + E(-a,-a,a)], \tag{14}$$

with $a = L/\sqrt{2}$, and

$$E(\alpha,\beta,\gamma) \equiv \frac{\mathrm{e}^{-\mathrm{i}/2(\alpha k_x+\beta k_y+\gamma k_z)}}{(\alpha k_x+\beta k_y)(\alpha k_x+\gamma k_z)(\beta k_y+\gamma k_z)}. \tag{15}$$

The lack of an inversion center causes the shape amplitude to be a complex quantity.

- *Regular hexagonal plate*: The shape amplitude of a regular hexagonal plate can be computed analytically, starting from Eq. (6) in Ref. [7], or, alternatively, by application of a six-fold rotation operation to the shape amplitude of a $60^\circ$ isosceless triangular plate, as described in Ref. [7]. The resulting expression for a plate with thickness $2c$ and edge length $2a$ (Fig. 1e) is given by:

$$D(\mathbf{k}) = \frac{2V}{3}\frac{\mathrm{sinc}(ck_z)}{k_x^2+k_y^2}\left[k_y^2\mathrm{sinc}(ak_x)\mathrm{sinc}(2a\delta k_y) + \sum_{j=1}^{2}\left(p_j\delta k_x + \frac{1}{2}k_y\right)^2\mathrm{sinc}\left[a\left(-\frac{p_j}{2}k_x + \delta k_y\right)\right]\mathrm{sinc}[2a\delta(p_j\delta k_x + \frac{1}{2}k_y)]\right], \tag{16}$$

where $\eta \equiv c/a$, $\delta \equiv \sqrt{3}/2$, and $p_j \equiv \{+1,-1\}$. The volume is equal to $V = 24\delta a^2 c$. When $k_x^2 + k_y^2 = 0$, the shape amplitude is given by

$$D(0,0,k_z) = V\mathrm{sinc}(ck_z). \tag{17}$$

This last expression is valid for all plate-like shapes with major surfaces normal to the $z$-direction.

- *Truncated paraboloid*: Consider a paraboloid oriented along the $z$-axis of a cartesian reference frame. The top of the paraboloid is in the origin, and the height is equal to $h = aR^2$, with $R$ the radius of the circle in the truncation plane (Fig. 1g). The shape amplitude (in cylindrical coordinates) consists of two terms:

$$D(\mathbf{k}) = \frac{2\pi\mathrm{i}R}{k_\perp k_z}\mathrm{e}^{-\mathrm{i}hk_z}J_1(k_\perp R) - \frac{2\pi\mathrm{i}}{k_z}\int_0^R J_0(k_\perp\rho)\rho\mathrm{e}^{-\mathrm{i}k_z\rho^2 a}\,\mathrm{d}\rho. \tag{18}$$

The radial integral can be solved by means of the following standard integral [8]:

$$\int_0^1 \mathrm{d}\rho\,\rho\mathrm{e}^{\mathrm{i}/2u\rho^2}J_0(vx) = \frac{1}{2}[L(u,v) + \mathrm{i}M(u,v)], \tag{19}$$

where $L(u,v)$ and $M(u,v)$ can be expressed in terms of the Lommel functions of two variables:

$$\frac{u}{2}L(u,v) = \sin\frac{v^2}{2u} + V_0(u,v)\sin\frac{u}{2} - V_1(u,v)\cos\frac{u}{2} \qquad (u > v); \tag{20}$$

$$= U_1(u,v)\cos\frac{u}{2} + U_2(u,v)\sin\frac{u}{2} \qquad (u<v); \tag{21}$$

$$\frac{u}{2}M(u,v) = \cos\frac{v^2}{2u} + V_0(u,v)\cos\frac{u}{2} - V_1(u,v)\sin\frac{u}{2} \qquad (u>v); \tag{22}$$

$$= U_1(u,v)\sin\frac{u}{2} - U_2(u,v)\cos\frac{u}{2} \qquad (u<v), \tag{23}$$

with

$$U_v(u,v) \equiv \sum_{k=0}^{\infty}(-1)^k\left(\frac{u}{v}\right)^{2k+v} J_{2k+v}(v), \tag{24}$$

$$V_v(u,v) \equiv \sum_{k=0}^{\infty}(-1)^k\left(\frac{v}{u}\right)^{2k+v} J_{2k+v}(v). \tag{25}$$

Introducing dimensionless variables $K_z \equiv hk_z$ and $K_\perp \equiv Rk_\perp$ we find for the shape amplitude of the truncated paraboloid:

$$D(K_\perp, K_z) = \frac{4V\mathrm{i}}{K_z}\left[\mathrm{e}^{-\mathrm{i}K_z}\frac{J_1(K_\perp)}{K_\perp} - \frac{1}{2}[L(2K_z, K_\perp) - \mathrm{i}M(2K_z, K_\perp)]\right], \tag{26}$$

where $V = \pi/2hR^2$ is the volume of the truncated paraboloid. The limiting cases for $K_z \to 0$ and $K_\perp \to 0$ can be computed easily by using only the lowest order terms of Eqs. (24) and (25). We find:

$$D(K_\perp, 0) = \frac{4V}{K_\perp}\left[J_1(K_\perp) - \frac{2}{K_\perp}J_2(K_\perp)\right], \tag{27}$$

$$D(0, K_z) = \frac{2V\mathrm{i}}{K_z}\left[\mathrm{e}^{-\mathrm{i}K_z} + \frac{\mathrm{i}}{2K_z}(1 + \mathrm{e}^{\mathrm{i}K_z})\right], \tag{28}$$

$$D(0,0) = V. \tag{29}$$

- *Cone truncated by spherical cap*: The shape amplitude for a cone with opening angle $\alpha$, truncated by a spherical cap of radius $R$ (Fig. 1h) is given by (in spherical coordinates):

$$D(\mathbf{k}) = 2\pi\sum_{l=0}^{\infty}(-\mathrm{i})^l[P_{l-1}(\cos\alpha) - P_{l+1}(\cos\alpha)]P_l(\cos\theta)\kappa_l(k,R), \tag{30}$$

with $P_l(x)$ the a Legendre polynomial, and

$$\kappa_l(k,R) \equiv \int_0^R \mathrm{d}\rho\, \rho^2 j_l(k\rho).$$

This radial integral can be rewritten as

$$\kappa_l(k,R) = \sqrt{\frac{\pi}{2k^3}}\int_0^{kR} \mathrm{d}x\, x^{\frac{3}{2}} J_{l+\frac{1}{2}}(x).$$

Using the relations

$$j_{l-1}(x) + j_{l+1}(x) = \frac{2l+1}{x} j_l(x)$$

and

$$\int \mathrm{d}x\, x^{\lambda} J_{\nu}(x) = x^{\lambda} J_{\nu+1}(x) - (\lambda - \nu - 1) \int \mathrm{d}x\, x^{\lambda-1} J_{\nu+1}(x)$$

we can derive the following recursion relation:

$$\kappa_{l+2}(k,R) = \frac{l+3}{l}\kappa_l(k,R) - \frac{2l+3}{l}\sqrt{\frac{\pi}{2}}\left(\frac{R}{k}\right)^{3/2} J_{l+\frac{3}{2}}(kR) \tag{31}$$

This recursion relation can be started if the integrals $\kappa_q(k,R)$ with $q = 0, \ldots, 2$ are known. They can be derived from equations [1.8.1.6] and [1.8.1.8] in Ref. [9]:

$$\kappa_0(k,R) = \frac{1}{k^3}[\sin(kR) - kR\cos(kR)]; \tag{32}$$

$$\kappa_1(k,R) = \frac{1}{k^3}[2 - 2\cos(kR) - kR\sin(kR)]; \tag{33}$$

$$\kappa_2(k,R) = \frac{1}{k^3}\left[kR\cos(kR) - 4\sin(kR) + 3\left(\mathrm{si}(kR) + \frac{\pi}{2}\right)\right], \tag{34}$$

with $\mathrm{si}(x) = \int_0^x (\sin t/t)\mathrm{d}t$ the sine integral.

This concludes the enumeration of shape amplitudes for a series of important particle shapes. In the following section, we will first derive a general expression for shapes of cylindrical symmetry, and then apply the formalism to the uniformly magnetized cylinder.

## 4. The demagnetization tensor field for objects with cylindrical symmetry

### 4.1. General theory

Consider a general object with cylindrical symmetry, as shown in Fig. 2. The top and bottom surfaces are assumed to be flat at $z = h_1$ and $h_2$. The object has an external surface described by $r = r_2(z)$, and an

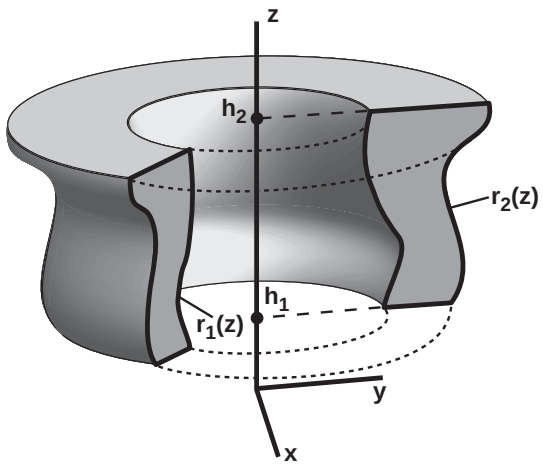


Fig. 2. Schematic representation of a general object of revolution with distinct inner and outer surfaces $r_s(z)$ and $r_2(z)$.

internal surface at $r = r_1(z)$. It is possible for $r_1(h_i)$ to be equal to $r_2(h_i)$ for one or both points. Both functions $r_i(z)$ are assumed to be single valued functions. The demagnetization tensor for such an object can be expressed by first determining the shape amplitude $D(\mathbf{k})$, which, in cylindrical coordinates with $\mathbf{k} = (k_\perp, \theta, k_z)$ and $\mathbf{r} = (r, \theta', z)$, is given by:

$$\begin{aligned} D(\mathbf{k}) &= \int_{h_1}^{h_2} \mathrm{d}z\, \mathrm{e}^{-\mathrm{i}zk_z} \int_{r_1(z)}^{r_2(z)} \mathrm{d}r\, r \int_0^{2\pi} \mathrm{d}\theta\, \mathrm{e}^{-\mathrm{i}k_\perp r\cos(\theta-\theta')}; \\ &= 2\pi \int_{h_1}^{h_2} \mathrm{d}z\, \mathrm{e}^{-\mathrm{i}zk_z} \int_{r_1(z)}^{r_2(z)} \mathrm{d}r\, rJ_0(k_\perp r); \\ &= \frac{2\pi}{k_\perp} \int_{h_1}^{h_2} \mathrm{d}z f(k_\perp, z)\mathrm{e}^{-\mathrm{i}zk_z}, \end{aligned} \tag{35}$$

with

$$f(k_\perp, z) \equiv r_2(z)J_1(k_\perp r_2(z)) - r_1(z)J_1(k_\perp r_1(z)). \tag{36}$$

The demagnetization tensor for this class of objects can be obtained by inserting the integral (35) into Eq. (4), expressed in cylindrical coordinates. The resulting four-fold integral is given by

$$N_{ij}(r, \theta', z') = \frac{1}{4\pi^2} \int_{h_1}^{h_2} \mathrm{d}z \int_0^{\infty} \mathrm{d}k_\perp f(k_\perp, z) \int_0^{2\pi} \mathrm{d}\theta\, \mathrm{e}^{\mathrm{i}k_\perp r\cos(\theta-\theta')} \int_{-\infty}^{+\infty} \mathrm{d}k_z \frac{k_i k_j \mathrm{e}^{-\mathrm{i}(z-z')k_z}}{k_\perp^2 + k_z^2}. \tag{37}$$

Inserting the Cartesian components of $\mathbf{k} = (k_\perp \cos\theta', k_\perp \sin\theta', k_z)$, and using the following standard integrals:

$$\int_0^{\pi} \mathrm{e}^{\mathrm{i}\beta\cos x}\cos(nx)\mathrm{d}x = \mathrm{i}^n \pi J_n(\beta) \qquad [3.915.2]; \tag{38}$$

$$\int_0^{\pi} \mathrm{e}^{\mathrm{i}\beta\cos x}\sin^{2v}(x)\mathrm{d}x = \sqrt{\pi}\left(\frac{2}{\beta}\right)^{v} \Gamma(v + \frac{1}{2})J_v(\beta) \qquad [3.915.5]; \tag{39}$$

$$\int_0^{\pi} \mathrm{e}^{z\cos x}\mathrm{d}x = \pi I_0(z) \qquad [3.339^6]; \tag{40}$$

where the numbers between square brackets refer to Ref. [10], the 6 independent components of the tensor $N_{ij}$ can be written as:

$$\begin{pmatrix} N_{11} \\ N_{22} \\ N_{33} \\ N_{12} \\ N_{13} \\ N_{23} \end{pmatrix} (r, \theta', z') = \frac{1}{4\pi} \int_{h_1}^{h_2} \mathrm{d}z \int_0^{\infty} \mathrm{d}k_\perp f(k_\perp, z) \begin{pmatrix} k_\perp^2 \left[J_0(k_\perp r) - \cos 2\theta' J_2(k_\perp r)\right] \\ k_\perp^2 \left[J_0(k_\perp r) + \cos 2\theta' J_2(k_\perp r)\right] \\ 2J_0(k_\perp r) \\ -\frac{1}{2}k_\perp^2 \sin 2\theta' J_2(k_\perp r) \\ 2\mathrm{i}k_\perp \cos\theta' J_1(k_\perp r) \\ 2\mathrm{i}k_\perp \sin\theta' J_1(k_\perp r) \end{pmatrix} \int_{-\infty}^{+\infty} \mathrm{d}k_z \begin{pmatrix} 1 \\ 1 \\ k_z^2 \\ 1 \\ k_z \\ k_z \end{pmatrix} \frac{\mathrm{e}^{-\mathrm{i}(z-z')k_z}}{k_\perp^2 + k_z^2}. \tag{41}$$

The integral over $k_z$ can be solved using the standard integrals [3.723.2], [3.723.3], and [3.738.2] in Ref. [10] and the demagnetization tensor is written as

$$N_{ij}(r, \theta', z') = \int_0^{\infty} \mathrm{d}k_\perp\, k_\perp S_{ij}(k_\perp, r, \theta') \int_{h_1}^{h_2} \mathrm{d}z f(k_\perp, z)\xi_{ij}^{(\pm)}\mathrm{e}^{\pm(z'-z)k_\perp}, \tag{42}$$

where

$$S_{ij}(k_\perp, r, \theta') \equiv \sum_{\mu=0}^{2} \alpha_{ij}^{(\mu)} J_\mu(k_\perp r), \tag{43}$$

and the matrices $\alpha_{ij}^{(\mu)}$ and $\xi_{ij}^{(\pm)}$ are defined as

$$\alpha_{ij}^{(0)} \equiv \frac{1}{4}\begin{pmatrix} 1 & 0 & 0 \\ 0 & 1 & 0 \\ 0 & 0 & 2 \end{pmatrix}, \qquad \alpha_{ij}^{(1)} \equiv \frac{1}{2}\begin{pmatrix} 0 & 0 & \cos\theta' \\ 0 & 0 & \sin\theta' \\ \cos\theta' & \sin\theta' & 0 \end{pmatrix}$$

$$\alpha_{ij}^{(2)} \equiv \frac{1}{8}\begin{pmatrix} -2\cos 2\theta' & \sin 2\theta' & 0 \\ \sin 2\theta' & 2\cos 2\theta' & 0 \\ 0 & 0 & 0 \end{pmatrix}, \qquad \xi_{ij}^{(\pm)} \equiv \begin{pmatrix} 1 & -1 & \pm 1 \\ -1 & 1 & \pm 1 \\ \pm 1 & \pm 1 & -1 \end{pmatrix}$$

The top sign in Eq. (42) is used when $z - z' > 0$, the bottom sign when $z - z' < 0$.

The main advantage of expression (42) is that there remain only 2 integrations compared to the 6 integrations needed to go from $D(\mathbf{r})$ to $N_{ij}(\mathbf{r})$. In some cases, one of the two integrals can be carried out analytically, leaving only one integral to be evaluated numerically. In the case of the cylinder, both integrals can be computed analytically, as shown explicitly in Section 4.2.

### 4.2. The demagnetization tensor field for the finite cylinder

The radial functions $r_i(z)$ for the cylinder result in the following expression for the function $f(k_\perp, z)$:

$$f(k_\perp, z) = RJ_1(k_\perp R), \tag{44}$$

which does not depend on the coordinate $z$. If we scale all coordinates by the cylinder radius $R$ ($\rho \equiv r/R$, $\zeta \equiv z'/R$, $\tau \equiv d/R$, and $K \equiv kR$), then the $z$-integral can be solved trivially (distinguishing between the regions $z' < -d$, $-d < z' < d$, and $d < z'$). The resulting expression for the demagnetization tensor is given by

$$N_{ij}(\rho, \theta', \zeta) = \int_0^\infty \mathrm{d}K\, S_{ij}(K, \rho, \theta') J_1(K) \begin{cases} 2\mathrm{e}^{-\zeta K}\sinh(\tau K)\xi_{ij}^{(-)} & [\tau < \zeta] \\ \xi_{ij}^{(-)}(1 - \mathrm{e}^{-(\tau+\zeta)K}) + \xi_{ij}^{(+)}(1 - \mathrm{e}^{-(\tau-\zeta)K}) & [-\tau < \zeta < \tau] \\ 2\mathrm{e}^{\zeta K}\sinh(\tau K)\xi_{ij}^{(+)} & [\zeta < -\tau] \end{cases} \tag{45}$$

Next we replace the hyperbolic function by exponential functions, and introduce the following notation:

$$\alpha_- \equiv |\zeta - \tau|, \tag{46}$$

$$\alpha_+ \equiv |\zeta + \tau|, \tag{47}$$

and

$$H_{\tau\zeta} = \begin{cases} 1 & \text{if } \tau > \zeta \\ 0 & \text{if } \tau < \zeta \end{cases} \qquad \text{and} \qquad s_{\tau\zeta} = \begin{cases} 1 & \text{if } \tau < \zeta \\ -1 & \text{if } \tau > \zeta \end{cases}$$

After some elementary manipulations we arrive at

$$\begin{aligned} N_{ij}(\rho, \theta', \zeta) = {} & \alpha_{ij}^{(2)}\left[s_{\zeta\tau} I_2(\rho, \alpha_-) + I_2(\rho, \alpha_+) - 2H_{\tau\zeta} I_2(\rho, 0)\right] \\ & - \alpha_{ij}^{(0)}\left[s_{\zeta\tau} I_0(\rho, \alpha_-) + I_0(\rho, \alpha_+) - 2H_{\tau\zeta}(1 - \delta_{i3}\delta_{j3}) I_0(\rho, 0)\right] \\ & - \alpha_{ij}^{(1)} s_{0\zeta}(I_1(\rho, \alpha_-) - I_1(\rho, \alpha_+)), \end{aligned} \tag{48}$$

where $\delta_{ij}$ is the identity matrix and

$$I_\mu(\rho,\alpha) \equiv \int_0^\infty \mathrm{d}K\, J_\mu(K\rho)J_1(K)\mathrm{e}^{-\alpha K}, \tag{49}$$

The integrals $I_\mu(\rho,\alpha)$ in Eq. (49) belong to the large class of Lipschitz–Hankel integrals involving the products of Bessel functions. There is a long history in the mathematical literature regarding this type of integral (e.g., [11,12]). We will follow Eason et al. [12] and express the integrals in terms of complete and incomplete elliptic integrals. To avoid confusion between the various notational schemes in use for elliptic integrals, we will use the definitions and notations as defined in the *Handbook of Mathematical Functions* by Abramowitz and Stegun [13, Chapter 17].

The solutions to the integrals of type (49) for $\alpha_\pm \neq 0$ are given by [9,12]

$$I_\mu(\rho,\alpha_\pm) = \begin{cases} s_{\rho 1}\dfrac{1}{2}\Lambda_0(\beta_\pm\backslash\kappa_\pm) - \dfrac{k_\pm\alpha_\pm}{2\pi\rho^{\frac{1}{2}}}K(m_\pm) + H_{\rho 1} & \text{for}\mu = 0, \\ \dfrac{1}{\pi k_\pm\sqrt{\rho}}\{(2-m_\pm)K(m_\pm) - E(m_\pm)\} & \text{for}\mu = 1, \\ \dfrac{2\alpha_\pm}{\pi k_\pm\rho^{3/2}}E(m_\pm) - \dfrac{\alpha_\pm k_\pm(\alpha_\pm^2+\rho^2+2)}{2\pi\rho^{\frac{5}{2}}}K(m_\pm) + & \\ s_{1\rho}\dfrac{1}{2\rho^2}\Lambda_0(\beta_\pm\backslash\kappa_\pm) + \dfrac{H_{1\rho}}{\rho^2} & \text{for}\mu = 2, \end{cases} \tag{50}$$

where

$$\beta_\pm = \sin^{-1}\left(\frac{\alpha_\pm}{\sqrt{(\rho-1)^2+\alpha_\pm^2}}\right) \quad \text{and}$$
$$m_\pm = k_\pm^2 = \sin^2\kappa_\pm = \frac{4\rho}{(\rho+1)^2+\alpha_\pm^2} \tag{51}$$

$K(m)$ and $E(m)$ are the complete elliptic integrals of the first and second kinds, respectively, and $\Lambda_0(\beta\backslash\kappa)$ is Heuman's Lambda function, which is defined as

$$\Lambda_0(\beta\backslash\kappa) = \frac{2}{\pi}\big(K(m)E(\beta\backslash 90^\circ - \kappa) - [K(m) - E(m)]F(\beta\backslash 90^\circ - \kappa)\big), \tag{52}$$

where $m \equiv \sin^2\kappa$. $E(\beta\backslash\alpha)$ and $F(\beta\backslash\alpha)$ are the (incomplete) elliptic integrals of the first and second kinds, respectively. The solutions to the integrals of type (49) for $\alpha_\pm = 0$ are given by [10]

$$I_0(\rho,0) = (1-\delta_{\rho 1})H_{1\rho} + \frac{1}{2}\delta_{\rho 1}, \tag{53}$$

$$I_2(\rho,0) = (1-\delta_{\rho 1})\frac{H_{\rho 1}}{\rho^2} + \frac{1}{2}\delta_{\rho 1}. \tag{54}$$

The solutions above are in agreement with those reported by Kraus [1] and Chen et al. [14].

We will now consider the eigenvalues and eigenvectors of the demagnetization tensor field. It is instructive to convert the cartesian tensor elements to their cylindrical equivalents, using the following

relations:

$$N_{rr}(\rho,\zeta) = N_{xx}(\rho,0,\zeta),$$
$$N_{zz}(\rho,\zeta) = N_{zz}(\rho,0,\zeta),$$
$$N_{rz}(\rho,\zeta) = N_{xz}(\rho,0,\zeta). \tag{55}$$

The component $N_{\theta\theta}(\rho,\zeta)$ follows from the trace condition on the tensor

$$N_{rr}(\rho,\zeta) + N_{\theta\theta}(\rho,\zeta) + N_{zz}(\rho,\zeta) = D(\rho,\zeta), \tag{56}$$

where $D$ is the cylinder shape function. The cylindrical symmetry means that there must be at least a $\infty m$ symmetry, i.e., a rotation axis of infinite order along $z$, with an infinite number of mirror planes containing the $z$ axis. This in turn means that two of the eigenvectors in any given point $\mathbf{r}$ must lie in the plane containing the $z$-axis and going through this point. Using the position dependent cylindrical basis vectors $\mathbf{e}_\rho$, $\mathbf{e}_\theta$, and $\mathbf{e}_z$, the eigenvectors are then expressed as:

$$\mathbf{E}_1 = (\cos\eta, 0, \sin\eta),$$
$$\mathbf{E}_2 = (0, 1, 0),$$
$$\mathbf{E}_3 = (-\sin\eta, 0, \cos\eta),$$

where $\eta$ is an angle to be determined (depends on $r$ and $z$). If we represent the eigenvalues by $\lambda_i$, then we can use the spectral decomposition to write down the explicit expression for the $N_{ij}$-tensor in cylindrical coordinates in the plane $\theta = 0$

$$N_{ij} = \begin{pmatrix} \cos\eta & 0 & -\sin\eta \\ 0 & 1 & 0 \\ \sin\eta & 0 & \cos\eta \end{pmatrix} \begin{pmatrix} \lambda_1 & 0 & 0 \\ 0 & \lambda_2 & 0 \\ 0 & 0 & \lambda_3 \end{pmatrix} \begin{pmatrix} \cos\eta & 0 & \sin\eta \\ 0 & 1 & 0 \\ -\sin\eta & 0 & \cos\eta \end{pmatrix},$$
$$= \begin{pmatrix} \lambda_1\cos^2\eta + \lambda_3\sin^2\eta & 0 & \cos\eta\sin\eta(\lambda_1 - \lambda_3) \\ 0 & \lambda_2 & 0 \\ \cos\eta\sin\eta(\lambda_1 - \lambda_3) & 0 & \lambda_3\cos^2\eta + \lambda_1\sin^2\eta \end{pmatrix}.$$

Since the trace of this matrix must be equal to the shape function, we have $\lambda_2 = D(\mathbf{r}) - \lambda_1 - \lambda_3$; there are hence three unknowns: $\eta(r,z)$, $\lambda_1(r,z)$, and $\lambda_3(r,z)$.

It is easy to show that the eigenvalues $\lambda_i$ and the angle $\eta$ can be expressed in terms of the cylindrical tensor elements, as follows:

$$\lambda_1 = \frac{1}{2}(N_{rr} + N_{zz}) + \frac{N_{rz}}{\sin 2\eta},$$
$$\lambda_3 = \frac{1}{2}(N_{rr} + N_{zz}) - \frac{N_{rz}}{\sin 2\eta},$$
$$\eta = \frac{1}{2}\tan^{-1}\left(\frac{2N_{rz}}{N_{rr} - N_{zz}}\right).$$

If the shape function has an additional mirror plane normal to the $z$-axis (e.g. cylinder, torus, etc.), then the $N_{rz}$ element of the tensor must be an odd function of $z$. The above equations are valid for any object with cylindrical symmetry.

The tensor elements are shown as grayscale plots in Fig. 3 for a cylinder with unit aspect ratio: (a) through (c) correspond to $N_{rr}$, $N_{rz}$ and $N_{zz}$, resp.; (d) through (f) represent the eigenvalues $\lambda^- = \min(\lambda_1, \lambda_3)$, $\lambda^+ = \max(\lambda_1, \lambda_3)$, and $\lambda_2$. The largest variations of the eigenvalues occur near the edges and corners, where the shape function is discontinuous. The eigenvalues and eigenvectors can be used to create a graphical representation of the demagnetization tensor field $N_{ij}(\mathbf{r})$ [2]. The tensor is represented by a quadratic surface

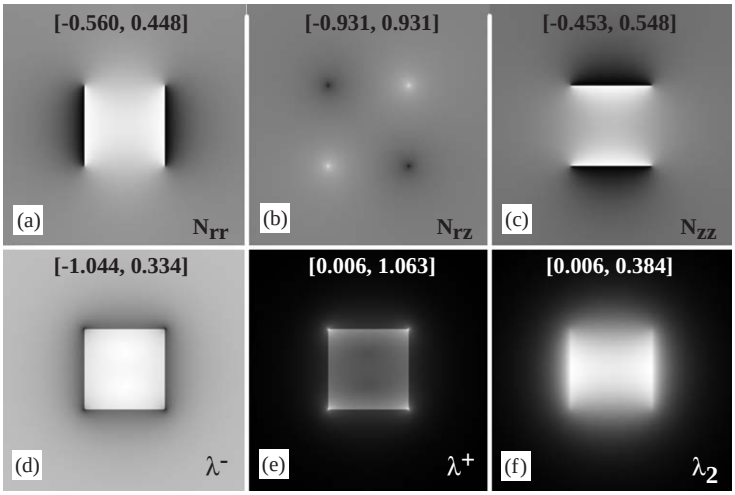


Fig. 3. Tensor elements for a cylinder with unit aspect ratio: $N_{rr}$ (a), $N_{rz}$ (b), and $N_{zz}$ (c). The corresponding eigenvalues $\lambda^-$, $\lambda^+$, and $\lambda_2$ are shown in (d) through (f), resp. The numbers near the top of each pattern correspond to the intensity scale: black is equal to the first number, white equals the second number.

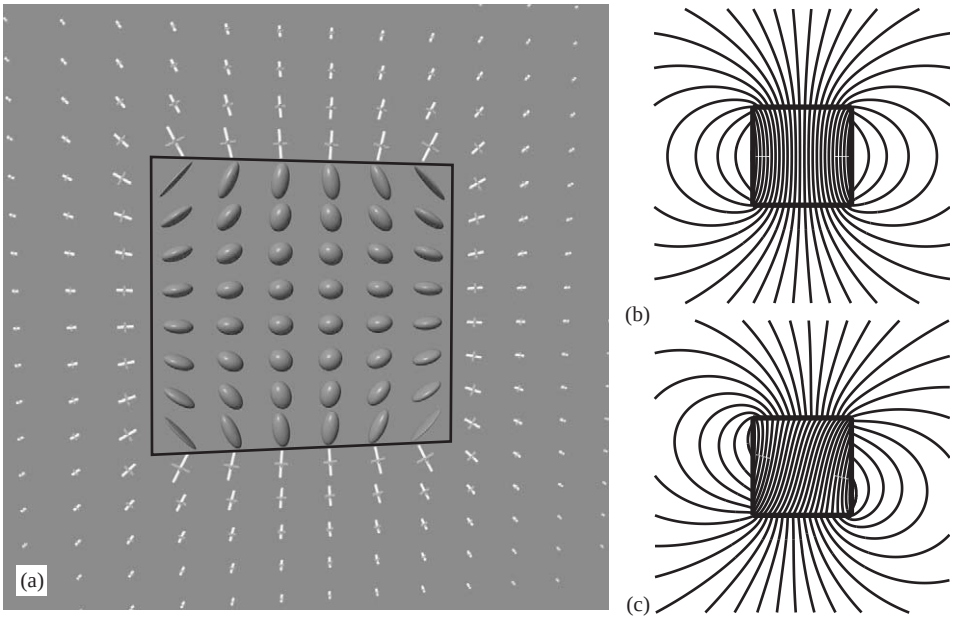


Fig. 4. (a) Three-dimensional perspective representation of the demagnetization tensor field in the plane $\theta = 0$ for a cylinder (outlined) with aspect ratio $\tau = 1$. The ellipsoids represent the demagnetization tensor in the interior of the cylinder. Intersections of three rods correspond to the eigenvectors of the demagnetization tensor outside the cylinder, with the light/dark colored rod being associated with the negative eigenvalue. When the tensor field is contracted with respect to a magnetization vector, the magnetic field **H** results. This can be combined with the magnetization vector to result in a field line plot of the magnetic induction **B**(**r**), as shown in (b) for **M** parallel to the cylinder axis, and in (c) for **M** at 15° from the cylinder axis.

with the eigenvectors along the main axes. For all points inside the cylinder, the eigenvalues are all positive, so that the resulting shape is an ellipsoid. For all points outside the cylinder, the trace of the tensor vanishes which means that one or two eigenvalues must be negative. This leads to single-sheet or double-sheet

hyperboloids, respectively. Fig. 4(a) shows a rendered drawing of the ellipsoids and single-sheet hyperboloids for a cylinder with unit aspect ratio; only points in the plane $\theta = 0$ are shown since all other planes are identical due to the cylindrical symmetry. The hyperboloids are represented by the intersection of three rods with the eigenvectors as directions and the eigenvalues as lengths. The negative eigenvalue is associated with the darker rod. From the ellipsoid representation one can derive the magnetic field $\mathbf{H}(\mathbf{r})$, and hence the magnetic induction, $\mathbf{B}(\mathbf{r})$, as described in Ref. [2]. As an example, the magnetic induction field lines for two different magnetization directions are shown in Fig. 4(b) and (c): in (b), the magnetization is parallel to the cylinder axis, whereas in (c), the magnetization is tilted 15° away from the cylinder axis.

## 5. The demagnetization energy for a finite cylinder

For a cylindrical disk with radius $R$ and thickness $t = 2d$, the shape amplitude is [4]

$$\frac{4\pi R}{k_\perp k_z} J_1(k_\perp R)\sin(dk_z), \tag{57}$$

with $k_\perp = \sqrt{k_x^2 + k_y^2}$ in the plane of the disk and the coordinate origin is taken at the center of the disk. Therefore, the demagnetization energy is given by the following integral:

$$E_m = \frac{\mu_0 M_0^2 R^2}{\pi} \int \mathrm{d}^3\mathbf{k} \frac{J_1(k_\perp R)^2}{(k_\perp^2 + k_z^2)k_\perp^2 k_z^2} \sin^2(dk_z)(\hat{\mathbf{m}} \cdot \mathbf{k})^2. \tag{58}$$

For a generic unit magnetization vector $(m_x, m_y, m_z)$, the scalar product $\mathbf{k} \cdot \hat{\mathbf{m}}$ is written as

$$\begin{aligned}(\mathbf{k} \cdot \hat{\mathbf{m}})^2 &= (m_x k_x + m_y k_y + m_z k_z)^2 \\ &= (\alpha + m_z k_z)^2 = \alpha^2 + 2\alpha m_z k_z + m_z^2 k_z^2,\end{aligned} \tag{59}$$

where $\alpha \equiv m_x k_x + m_y k_y$ is introduced for convenience. The integral is then

$$E_m = \frac{\mu_0 M_0^2 R^2}{\pi} \int_0^\infty \mathrm{d}k_\perp \frac{J_1(k_\perp R)^2}{k_\perp} \int_0^{2\pi} \mathrm{d}\theta \int_{-\infty}^{+\infty} \mathrm{d}k_z \frac{1}{k_\perp^2 + k_z^2} \frac{\sin^2(dk_z)}{k_z^2} (\alpha + m_z k_z)^2. \tag{60}$$

We first perform the integral along $k_z$. Considering that the integral containing the $2\alpha m_z k_z$ term of Eq. (18) is odd and hence vanishes, we have

$$\int_{-\infty}^{+\infty} \mathrm{d}k_z \frac{1}{k_\perp^2 + k_z^2} \frac{\sin^2(dk_z)}{k_z^2} (\alpha^2 + m_z^2 k_z^2) = \frac{\pi\alpha^2}{2k_\perp^3}(k_\perp t - 1 + \mathrm{e}^{-k_\perp t}) + \frac{\pi m_z^2}{2k_\perp}(1 - \mathrm{e}^{-k_\perp t}). \tag{61}$$

We may note that the only angular dependence is in $\alpha$, therefore the integration on $\theta$ gives

$$\begin{aligned}\int_0^{2\pi} \mathrm{d}\theta \alpha^2 &= k_\perp^2 \int_0^{2\pi} \mathrm{d}\theta (m_x^2 \cos^2\theta + m_y^2 \sin^2\theta + m_x m_y \sin 2\theta) \\ &= \pi k_\perp^2 (m_x^2 + m_y^2) = \pi k_\perp^2 (1 - m_z^2),\end{aligned} \tag{62}$$

and hence Eq. (61) becomes

$$\frac{\pi^2(1 - m_z^2)}{2k_\perp}(k_\perp t - 1 + \mathrm{e}^{-k_\perp t}) + \frac{2\pi^2 m_z^2}{2k_\perp}(1 - \mathrm{e}^{-k_\perp t}), \tag{63}$$

or, rearranging the terms

$$\frac{\pi^2}{2k_\perp}[(k_\perp t - 1 + \mathrm{e}^{-k_\perp t}) - m_z^2(k_\perp t - 3 + 3\mathrm{e}^{-k_\perp t})]. \tag{64}$$

We are then left with the following integral:

$$E_m = \frac{\pi\mu_0 M_0^2 R^2}{2} \int_0^\infty \mathrm{d}k_\perp \frac{J_1(k_\perp R)^2}{k_\perp^2}[(k_\perp t - 1 + \mathrm{e}_\perp^- t) - m_z^2(k_\perp t - 3 + 3\mathrm{e}^{-k_\perp t})], \tag{65}$$

which gives finally

$$E_m = \frac{\mu_0 M_0^2 R^2}{12}\left[8R(3m_z^2 - 1) + 6\pi t m_z^2 - 3\pi t(3m_z^2 - 1)_2F_1\left(-\frac{1}{2},\frac{1}{2};2;-\frac{4R^2}{t^2}\right)\right] \tag{66}$$

where the ${}_2F_1(a,b;c;z)$ function is a hypergeometric function. In terms of the $\tau = t/2R$ ratio, and introducing a different hypergeometric function from the following equality:

$${}_2F_1\left(-\frac{1}{2},\frac{1}{2};2;-\frac{1}{\tau^2}\right) = \frac{1}{\tau}\sqrt{1+\tau^2}\,{}_2F_1\left(-\frac{1}{2},\frac{3}{2};2;\frac{1}{1+\tau^2}\right) \tag{67}$$

we arrive at

$$E_m = \frac{\mu_0 M_0^2 R^3}{6}\left[4(3m_z^2 - 1) + 6\pi\tau m_z^2 - 3\pi\sqrt{1+\tau^2}(3m_z^2 - 1)_2F_1\left(-\frac{1}{2},\frac{3}{2};2;\frac{1}{1+\tau^2}\right)\right] \tag{68}$$

We can normalize the entire energy expression by introducing the particle volume $V$ and defining:

$$E_m' \equiv \frac{E_m}{\mu_0 M_0^2 V} = \frac{1}{2}m_z^2 + \frac{3m_z^2 - 1}{\tau}\left[\frac{1}{3\pi} - \frac{\sqrt{1+\tau^2}}{4}\,{}_2F_1\left(-\frac{1}{2},\frac{3}{2};2;\frac{1}{1+\tau^2}\right)\right] \tag{69}$$

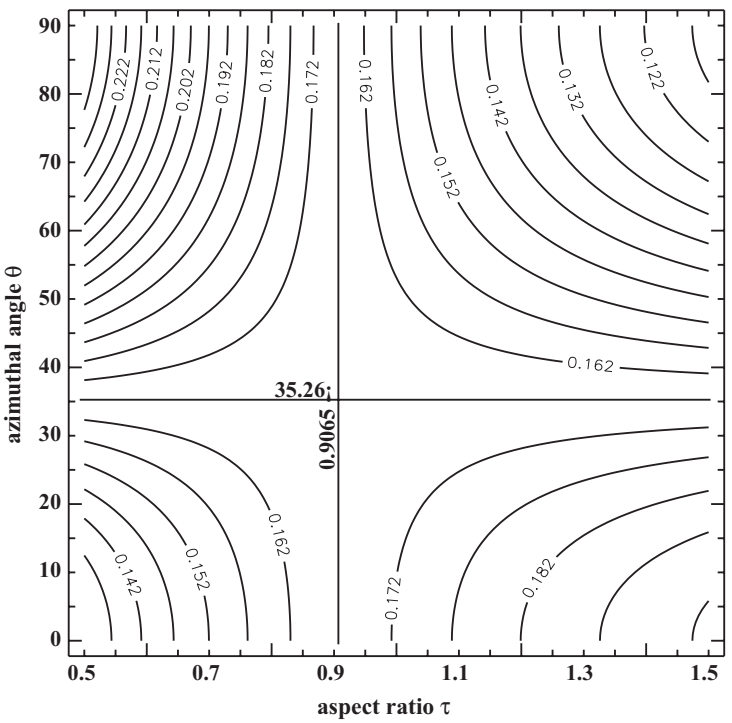


Fig. 5. Reduced energy $E_m'$ as a function of the aspect ratio $\tau$ and the azimuthal angle $\theta$ for the uniformly magnetized cylinder. The saddle surface is centered at the location $(0.9065, 35.26^\circ)$, where $E_m' = \frac{1}{6}$.

This function becomes a constant ($E'_m = 1/6$, independent of $\tau$) for $m_z^2 = 1/3$, which corresponds to an angle of 35.26° for $\theta$. However, this is not a stable configuration, as the energy reaches always an absolute minimum or maximum either for $m_z = 0$ (in plane magnetization) or $m_z = 1$ (vertical magnetization). The transition between the two states is reached for an aspect ratio $\tau = 0.9065$, showing that for a flat disk shape ($t \ll R$) the in-plane magnetization is favorable, while for a rod shape ($t \gg R$) the vertical magnetization is favorable. The energy $E'_m$ is shown as a function of the aspect ratio $\tau$ and the azimuthal angle $\theta$ in Fig. 5. Along the straight horizontal and vertical straight lines we have $E'_m = \frac{1}{6}$.

## 6. The magnetometric demagnetization tensor for a finite cylinder

Combining Eqs. (8) and (57) we have for the magnetometric demagnetization tensor

$$\langle N \rangle_{ij} = \frac{2R^2}{\pi V} \int \mathrm{d}^3\mathbf{k} \frac{J_1^2(k_\perp R)\sin^2(dk_z)}{k_\perp^2 k_z^2 (k_\perp^2 + k_z^2)} k_i k_j. \tag{70}$$

Solving for the angular integrals one can show that only the diagonal elements of the volume averaged tensor can be non-zero:

$$\begin{pmatrix} \langle N \rangle_{11} \\ \langle N \rangle_{22} \\ \langle N \rangle_{33} \end{pmatrix} = \frac{2R^2}{V} \int_0^\infty \frac{\mathrm{d}k_\perp}{k_\perp} \begin{pmatrix} k_\perp^2 \\ k_\perp^2 \\ 2 \end{pmatrix} J_1^2(k_\perp R) \int_{-\infty}^{+\infty} \mathrm{d}k_z \frac{\sin^2(dk_z)}{k_z^2(k_\perp^2 + k_z^2)} \begin{pmatrix} 1 \\ 1 \\ k_z^2 \end{pmatrix}. \tag{71}$$

The integrals over $k_z$ can be solved by means of equations [3.826.1] and [3.824.1] in Ref. [10]. Using

$$\int_0^\infty \mathrm{d}k_\perp \frac{J_1^2(k_\perp R)}{k_\perp} = \frac{1}{2} \quad \text{and}$$
$$\int_0^\infty \mathrm{d}k_\perp \frac{J_1^2(k_\perp R)}{k_\perp^2} = \frac{4}{3\pi}, \tag{72}$$

we can rewrite the diagonal elements of the volume averaged tensor as:

$$\langle N \rangle_{ii} = \begin{pmatrix} \frac{1}{2} \\ \frac{1}{2} \\ 0 \end{pmatrix} - \frac{1}{2\tau} \begin{pmatrix} 1 \\ 1 \\ -2 \end{pmatrix} \left[ \frac{4}{3\pi} - \int_0^\infty \mathrm{d}K \frac{J_1^2(K)}{K^2} \mathrm{e}^{-2\tau K} \right], \tag{73}$$

where we have introduced dimensionless coordinates. The integral over $K$ is again of the Lipschitz–Hankel type [12] and we find for the magnetometric demagnetization tensor of the uniformly magnetized finite cylinder:

$$\langle N \rangle_{ii} = \begin{pmatrix} \frac{1}{2} \\ \frac{1}{2} \\ 0 \end{pmatrix} - \frac{1}{2\tau} \begin{pmatrix} 1 \\ 1 \\ -2 \end{pmatrix} \left[ \frac{4}{3\pi} - \frac{4}{3\pi} \sqrt{1+\tau^2} (\tau^2 K(\kappa) + (1-\tau^2) E(\kappa)) + \tau \right], \tag{74}$$

with

$$\kappa^2 = \frac{1}{1+\tau^2}. \tag{75}$$

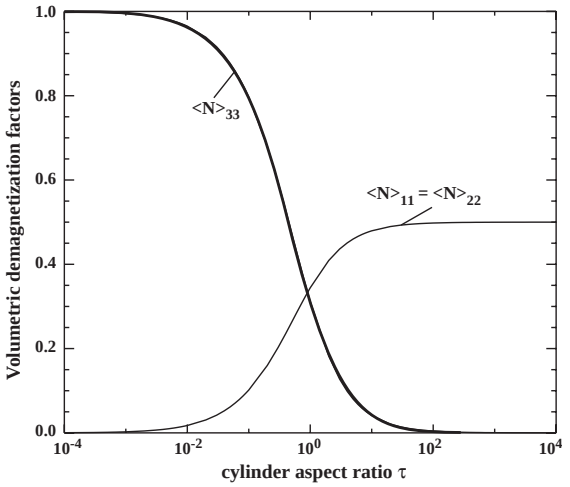


Fig. 6. Volumetric demagnetization factors for the finite cylinder as a function of the aspect ratio $\tau$ (logarithmic scale). The factors are equal to $\frac{1}{3}$ when $\tau = 0.9065$.

The limiting cases are easily derived from this expression: for $\tau \to \infty$, the second part of Eq. (74) vanishes, so that the magnetometric demagnetization factors are equal to $(\frac{1}{2}, \frac{1}{2}, 0)$. For $\tau \to 0$ the term between square brackets in Eq. (74) approaches $\tau$, so that the demagnetization factors are $(0, 0, 1)$. These cases correspond to the infinite cylinder and the infinite plane, respectively. Eq. (74) is in agreement with the results of Joseph et al. [15]; the magnetometric demagnetization factors for the finite cylinder are shown graphically in Fig. 6.

## 7. Applications

The formalism developed for the uniformly magnetized cylinder can be applied to study the magnetic field of a solenoid. In fact, a uniform magnetization over a cylindrical magnet is equivalent to a current flowing on the surface of the cylinder. We will now show how to extract some useful information which is not easily accessible by means of the standard real-space approach.

From Eq. (2) we have that the $z$ component of the **H**-field can be written explicitly as

$$H_z(r,z) = -\frac{M_0 R}{\pi} \int \frac{k_z \mathrm{d}k\, \mathrm{d}k_z}{k^2 + k_z^2} J_1(kR) J_0(kr) \sin(dk_z) \mathrm{e}^{\mathrm{i}zk_z}. \tag{76}$$

As a first easy result, we calculate the field at the center of the solenoid. For $r = 0$ and $z = 0$, after the integration in $k_z$, we obtain

$$H_z(0,0) = -M_0 \int \mathrm{d}K J_1(K) \mathrm{e}^{-\tau K}, \tag{77}$$

which, considering that within the solenoid the **M**-field is also present, results in

$$B_z(0,0) = B_0 \frac{\tau}{\sqrt{1+\tau^2}}. \tag{78}$$

Note that, in the limit $\tau \to \infty$, the field is $B_0$, which is the field of an infinite solenoid. On the other hand, for $\tau \to 0$, the field goes to zero, consistent with the results shown for the volume averaged demagnetizing tensor. For $\tau = 1$ we have $B_0/2$.

With a very similar argument, we may calculate the field along the solenoid axis, obtaining an analytical expression, which we will not report here. Instead, we give the expression for the field at the upper surface of the solenoid, which is

$$B_z(0,d) = B_0 \frac{\tau}{\sqrt{1+4\tau^2}}, \tag{79}$$

which is 0 for $\tau = 0$ and $B_0/2$ for $\tau \to \infty$.

It is also interesting to evaluate the external field of the solenoid. In fact, in order to evaluate to what extent we can consider a solenoid as "ideal", it is necessary to have information about the field just outside the lateral surface. We can evaluate directly from Eq. (76) the field at $r = R$ and $z = 0$

$$\begin{aligned} H_z(R,0) &= -M_0 \int \mathrm{d}K J_1(K) J_0(K) \mathrm{e}^{-\tau K} \\ &= -\frac{M_0}{2}\left[1 - \frac{2}{\pi} K\left(-\frac{4}{\tau^2}\right)\right], \end{aligned} \tag{80}$$

where $K(x)$ is the $K$-elliptic function [10]. The field goes from $-M_0/2$ for $\tau \to 0$, to zero for an infinite solenoid. Depending on the degree of ideality we desire for our solenoid, we can exploit the previous result to determine an acceptable aspect ratio. For instance, taking the value $\tau = 20$, we have an external field just outside the surface of the order of 0.1% of $M_0$, which can be considered in a good approximation as ideal.

Another simple calculation is the current loop. Taking the limit for $d \to 0$ in Eq. (76), we can calculate the field along the $z$-axis from

$$H_z(0,z) = -\frac{M_0 R d}{\pi} \int \frac{k_z^2 \mathrm{d}k \mathrm{d}k_z}{k^2 + k_z^2} J_1(kR) \mathrm{e}^{\mathrm{i}zk_z}, \tag{81}$$

which, after the integration in $k_z$ yields

$$\begin{aligned} H_z(0,z) &= \frac{M_0 R t}{2} \int k \mathrm{d}k J_1(kR) \mathrm{e}^{-k|z|} \\ &= \frac{M_0 R^2 t}{2} \frac{1}{(z^2+R^2)^{3/2}}. \end{aligned} \tag{82}$$

Considering the relationship between magnetic moment and current in a loop $\mu = M_0 V = IA$, where $A$ is the area of the loops, we can write $M_0 A t = IA$ or $M_0 t = I$, thus obtaining the Biot–Savart law

$$B_z(0,z) = \frac{\mu_0 I}{2} \frac{R^2}{(z^2+R^2)^{3/2}}. \tag{83}$$

As a final remark, it can be interesting to verify that, independent of the aspect ratio of the cylinder, the total flux of the **H**-field over the $z = 0$ plane is always equal (with opposite sign) to the flux enclosed in the solenoid. Writing Eq. (21) in cartesian coordinates, we obtain for $z = 0$:

$$\begin{aligned} \phi_H &= \int \mathrm{d}x \mathrm{d}y H_z(x,y,z) \\ &= -\frac{M_0 R}{2\pi^2} \int \frac{k_z \mathrm{d}^3\mathbf{k}}{k_\perp k^2} J_1(k_\perp R) \sin(dk_z) \int \mathrm{d}x\, \mathrm{d}y\, \mathrm{e}^{\mathrm{i}xk_x} \mathrm{e}^{\mathrm{i}yk_y}, \end{aligned} \tag{84}$$

which, considering the definition of the Dirac-$\delta$ distribution, and the limit $J_1(k_\perp R)/k_\perp = R/2$ for $k_\perp \to 0$, can be evaluated easily as

$$\phi_H = -M_0 R^2 \int \frac{\mathrm{d}k_z}{k_z} \sin(dk_z) = -M_0 \pi R^2, \tag{85}$$

which is exactly the solenoid magnetization multiplied by its cross section, as expected.

## 8. Conclusions

We have shown that the Fourier space shape amplitude formalism can be applied to the computation of the demagnetization tensor field of uniformly magnetized particles of arbitrary shape, and as an example we have derived the complete DTF for the cylinder with arbitrary aspect ratio. In addition, the magnetostatic energy and the volumetric demagnetization factors were derived in closed form. We have applied the formalism also to the computation of the magnetic field at various special points around a solenoid. An overview of numerical procedures which can be used to compute the DTF for more complex shapes will be presented in Part II of this paper [3].

## Acknowledgements

The authors would like to acknowledge stimulating interactions with J. Zhu, M. McHenry, and D. Laughlin. Financial support was provided by the US Department of Energy, Basic Energy Sciences, under contract numbers DE-FG02-01ER45893 and DE-AC02-98CH10886.

## References

[1] L. Kraus, Czech. J. Phys. B 23 (1973) 512.
[2] M. Beleggia, M. De Graef, J. Magn. Magn. Mater. 263 (2003) L1.
[3] S. Tandon, M. Beleggia, Y. Zhu, M. De Graef, J. Magn. Magn. Mater. (2004), this issue.
[4] M. Beleggia, Y. Zhu, Phil. Mag. B 83 (2003) 1143.
[5] J. Komrska, Optik 80 (1987) 171.
[6] J. Komrska, W. Neumann, Phys. Stat. Sol A 150 (1995) 89.
[7] M. Beleggia, S. Tandon, Y. Zhu, M. De Graef, Phil. Mag. B 83 (2003) 1143.
[8] K.D. Mielenz, J. Res. Natl. Inst. Stand. Technol. 103 (1998) 497.
[9] A.P. Prudnikov, Yu.A. Brychkov, O.I. Marichev, Integrals and Series, Volume 2: Special Functions, Gordon and Breach Science Publishers, London, 1998.
[10] I.S. Gradshteyn, I.M. Ryzhik, Tables of Integrals, Series and Products, Academic Press, New York, 2000.
[11] G.N. Watson, A Treatise on the Theory of Bessel Functions. 2nd Edition, Cambridge University Press, Cambridge, 1944.
[12] G. Eason, B. Noble, I.N. Sneddon, Philos. Trans. Roy. Soc. London A 247 (1955) 529–551.
[13] M. Abramozitz, I. Stegun, Handbook of Mathematical Functions, Dover Publications Inc., New York, 1972.
[14] D.-X. Chen, J.A. Brug, R.B. Goldfarb, IEEE Trans. Magn. 27 (1991) 3601.
[15] R.I. Joseph, J. Appl. Phys. 37 (1966) 4639.